Journal of Sulfur Chemistry
Publication details, including instructions for authors and subscription information:
http://www.informaworld.com/smpp/title~content=t713926081

Computational investigations on the electronic structure and reactivity of thiourea dioxide: sulfoxylate formation, tautomerism and dioxygen liberation

Zoltán Kis[a]; Sergei V. Makarov[b]; Radu Silaghi-Dumitrescu[a]
[a] Department of Chemistry and Chemical Engineering, Faculty of Chemistry and Chemical Engineering, 'Babes-Bolyai' University, Cluj-Napoca, Romania [b] State University of Chemistry and Technology, Ivanovo, Russia

Online publication date: 09 February 2010

To cite this Article Kis, Zoltán , Makarov, Sergei V. and Silaghi-Dumitrescu, Radu(2010) 'Computational investigations on the electronic structure and reactivity of thiourea dioxide: sulfoxylate formation, tautomerism and dioxygen liberation', Journal of Sulfur Chemistry, 31: 1, 27 — 39
To link to this Article: DOI: 10.1080/17415990903505902
URL: http://dx.doi.org/10.1080/17415990903505902

Journal of Sulfur Chemistry
Vol. 31, No. 1, February 2010, 27–39

Taylor & Francis
Taylor & Francis Group

Computational investigations on the electronic structure and reactivity of thiourea dioxide: sulfoxylate formation, tautomerism and dioxygen liberation

Zoltán Kis[a], Sergei V. Makarov[b] and Radu Silaghi-Dumitrescu[a]*

[a]*Department of Chemistry and Chemical Engineering, Faculty of Chemistry and Chemical Engineering, 'Babes-Bolyai' University, 11 Arany Janos Str., Cluj-Napoca RO-400028, Romania;* [b]*State University of Chemistry and Technology, Engels Str. 7, Ivanovo 153000, Russia*

(*Received 12 August 2009; final version received 21 November 2009*)

Thiourea dioxide, $(NH_2)_2CSO_2$ (TDO), is known to decompose in alkaline media to yield the strong reducing agent sulfoxylate, SO_2H^-, with interesting applications in (bio)catalysis. The electronic structure of TDO has been debated recently, with two different descriptions put forth based on crystal structures and electronic structure calculations, all gravitating around the unusually long C−S bond in TDO: a zwitterionic structure and a carbene one. Here, computational methods (density functional and Hartree–Fock) are used to reconcile the two descriptions. The geometrical parameters as well as the molecular orbitals and population analyses are all consistent with TDO being an adduct of SO_2 with the carbene $(NH_2)_2C$. The reactivity of TDO towards tautomerization, sulfoxylate formation and dioxygen liberation is also examined; all of the data points toward its tautomer, formamidine sulfinic acid (FSA), being the stable tautomer in solution, with TDO stabilized by supramolecular interactions in the solid state.

Keywords: thiourea dioxide; sulfoxylate; DFT; formamidine sulfinic acid; tautomer

1. Introduction

Thiourea-*S*,*S*-dioxide, $(NH_2)_2CSO_2$ (TDO), is a readily available stable water-soluble molecule, first prepared in 1910 by Barnett (*1*). There have been numerous commercial applications of its reducing property (and implicitly antioxidant, anticorrosive or bleaching), especially in the textile industry (*2*), bleaching of mechanical pulp (*3*), paper and leather-processing industries (*4*). TDO decomposes in alkaline conditions (with a $pK_a \sim 9.5$) generating sulfoxylate, a strong reducing agent, whose oxidation in turn yields dithionite, a common reducing agent in biochemistry (*4*, *5*). Paradoxically, besides liberating the strong reducing agents sulfoxylate and dithionite, TDO can also generate molecular oxygen, either at reflux in anhydrous acetonitrile (*6*) or in water in a narrow range of pH (*7*). A tautomeric form of TDO, formamidine sulfinic acid (FSA), is also known but has not been characterized structurally.

*Corresponding author. Email: rsilaghi@chem.ubbcluj.ro

ISSN 1741-5993 print/ISSN 1741-6000 online

DOI: 10.1080/17415990903505902
http://www.informaworld.com

We have recently demonstrated that TDO offers a new route towards carbon monoxide adducts of heme proteins, by the reduction in carbon dioxide (*5*). Evidence for TDO-based production of 'super-reduced' iron in myoglobin also exists (*5*). Catalytic properties of heme model complexes and related species in the presence of sulfoxylate have been demonstrated (*4, 8–11*). Furthermore, this strong reducing agent leads to formal oxidation states of Fe(0) and Fe(I) in iron-tetrasulfophthalocyanines in aqueous media (*11*).

Several X-ray diffraction structures of TDO are known (*12, 13*); together with molecular mechanics, *ab initio* and density functional theory (DFT), these data have been interpreted as evidence for a zwitterionic structure, $(H_4N_2C)^+(SO_2)^-$, with a remarkably long C−S bond, all consistent with the facile cleavage undergone in water at basic pH as outlined above. On the other hand, Denk *et al*. (*14*) characterized TDO as being the adduct of a carbene with sulfur dioxide, based on geometrical and energetical parameters derived from DFT.

Here computational chemistry calculation (DFT and Hartree–Fock) results are reported in order to elucidate the structure of TDO (zwitterionic *vs*. carbenoid), the nature of the unusually long C−S bond, the TDO–FSA tautomerism, the mechanism of sulfoxylate liberation and the mechanism of dioxygen liberation from TDO.

2. Results and discussion

2.1. *Structure of TDO*

Figure 1 shows optimized geometries for TDO, methanethiol (featuring a well-defined σ C−S bond), and thioformaldehyde (featuring a well-defined C−S double bond). A comparison of C−S bond lengths and electron densities reveals the C−S bond in TDO to be significantly longer/weaker than a normal C−S single bond.

Table 1 shows NBO partial atomic charges on TDO. It can be seen that there is only a small charge separation between the two moieties of TDO ($C(NH_2)_2$and SO_2); therefore, TDO does not appear to be well described by a zwitterionic structure. Moreover, when the C−S distance is increased to 4.1 Å (*i.e*. some 0.5 Å beyond the sum of the van der Waals radii of the two atoms), the small charge separation vanishes, instead of the increase expected of a zwitterionic structure. Consistent with this non-zwitterionic character, the TDO LUMO, shown in Figure 2, indicates a 'hole' on the TDO carbon, *i.e*. a formally empty 2p orbital corresponding to a singlet carbenoid structure.

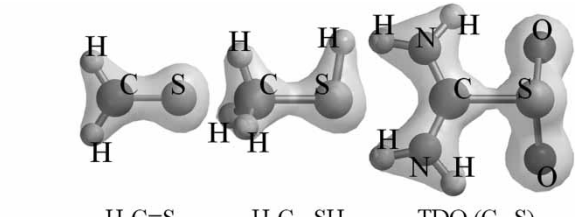

	$H_2C{=}S$	$H_3C{-}SH$	TDO (C–S)
B3LYP	1.62	1.85	1.99
BP	1.63	1.85	2.01
HF	1.60	1.83	1.90

Figure 1. Optimized structure of TDO and two reference systems, methanethiol and thioformaldehyde. Corresponding bond lengths, computed with different methods/functionals, are shown below each structure in angstroms. The transparent surfaces represent electron density, IsoVal = 0.12.

Table 1. NBO partial atomic charges on the TDO equilibrium structure and on the structure with TDO C−S distance of 4.1 Å.

Atom	TDO	Sum	C−S at 4.1 Å	Sum
S	1.52	−0.47	1.56	−0.03
O[a]	−0.98		−0.79	
C	0.31	+0.47	0.19	+0.03
N[b]	−0.81		−0.86	
H[c]	0.44		0.39	

Notes: [a]Same charge on both oxygen atoms. [b]Same charge on both nitrogen atoms. [c]Average charges of four hydrogen atoms.

2.2. *Structure of FSA*

Figure 3 shows the optimized structure of the FSA tautomer of TDO. The FSA C−S distance, at 1.89 Å, is 0.1 Å shorter than in TDO but still longer by 0.04 Å than a C−S single bond (*cf.* Figure 1).

The charge distribution of FSA (Table 2) differs fundamentally from that of TDO: the SO_2H moiety is now the positive 'pole' and the CN_2H_3 the negative one. This change in polarity is at odds with a zwitterionic character within FSA that would include a nascent sulfoxylate anion and is also consistent with the shorter C−S bond in FSA compared with TDO.

2.3. *TDO–FSA tautomerization*

A potential curve for intramolecular TDO−FSA tautomerization is shown in Figure 4. Clearly, the activation costs for tautomerization are very small starting either from FSA (∼6 kcal/mol) or from TDO (∼3.5 kcal/mol). At least in vacuum, FSA appears to be the more stable tautomer.

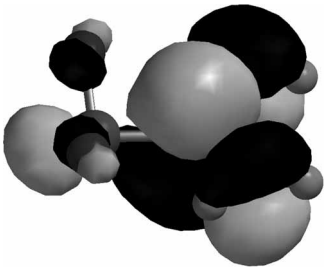

Figure 2. TDO LUMO.

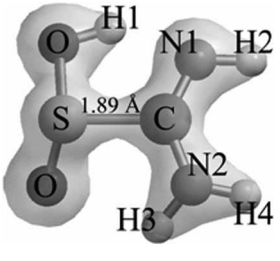

Figure 3. Optimized structure of FSA. Transparent surface represents the electron density, IsoVal = 0.12.

Table 2. Mulliken partial atomic charges on FSA and on the two moieties, SO_2H and CN_2H_3.

Atom	Charge	Sum
S	1.48	+0.15
O[a]	−0.92	
H1	0.52	
C	0.26	−0.15
N1	−0.78	
N2	−0.86	
H2	0.39	
H3	0.44	
H4	0.42	

Note: Labels are shown in Figure 3.

On the other hand, the potential curve for an intermolecular tautomerization is shown in Figure 5; an essentially all-planar 'head-to-tail' conformation (*cf.* Figure 5) was found to yield the lowest-energy pathway.

An alternative conformation to that seen in Figure 5, with the two TDO molecules on top of each other in a head to tail position, with four NH−O hydrogen bonds instead of the two hydrogen bonds shown in Figure 5, is preferred by 7.6 kcal/mol (structure shown in Figure 6). However, in this case, the hydrogen bonds are longer (∼1.9 Å) compared with the conformation in Figure 5 (∼1.6 Å); furthermore, consistent with this longer NH−O distance, proton migration and isomerization to FSA appear to entail a slightly larger energetical cost (∼9 kcal/mol (*cf.* Figure 6) compared with the 5 kcal/mol of Figure 5).

It is worth noting that the supramolecular arrangements shown in Figures 5 and 6 lead to stabilization of the TDO tautomer with respect to the FSA, in contrast to the situation seen in Figure 4 for isolated molecules *in vacuo*. This observation is consistent with the fact that crystallization has so far yielded only the TDO tautomer and never the FSA (*12–14*), while also suggesting that in dilute solutions and in the absence of strongly interacting hydrogen-bonding partners the FSA tautomer may also play an important role. The solvation energy (in water, Cosmo model) of TDO, FSA and the energy barrier for intra- and intermolecular tautomerization were computed also, and yielded results qualitatively similar to Figures 4–6, with the intramolecular pathway slightly favored but with all three barriers not higher than ∼10 kcal/mol. These values

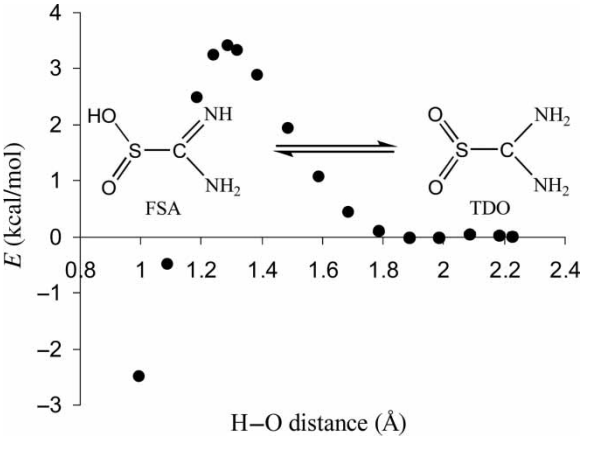

Figure 4. Potential curve for TDO−FSA intramolecular tautomerization in vacuum. One O−H distance was varied as shown, with all others parameters freely optimized.

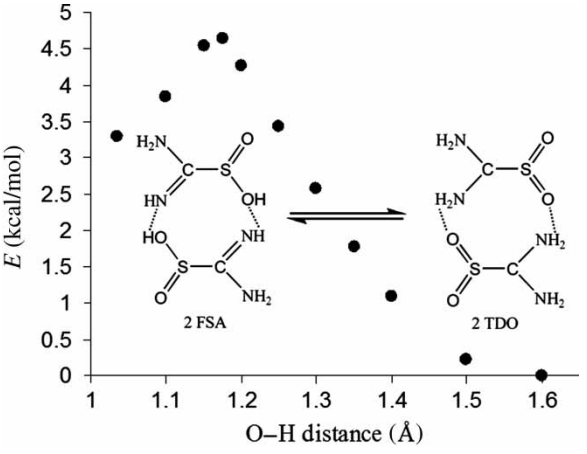

Figure 5. Potential curve for TDO−FSA intermolecular tautomerization in vacuum; two molecules of TDO/FSA were placed side by side in a head-to-tail position. One of the O−H distances was varied as shown, with all others parameters freely optimized.

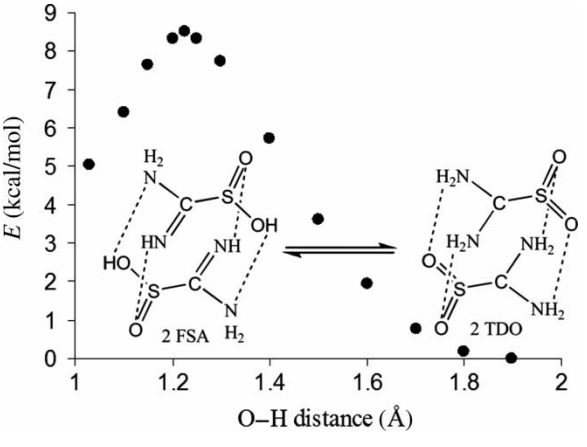

Figure 6. Potential curve for TDO−FSA intermolecular tautomerization in vacuum when two molecules of TDO/FSA were placed on the top of the other in a head-to-tail position. One of the O−H distances was varied as shown, with all other parameters freely optimized.

are extremely small and suggest that tautomerization would proceed at rates difficult to measure experimentally, by both intra- and intermolecular mechanisms.

Figure 7 shows HOMO for TDO and FSA. The relative stabilities of TDO and FSA are likely explained by the stabilizing effect of the intramolecular hydrogen bonds, which in FSA include a distinctly stronger interaction (1.84 Å in FSA vs. 2.2 Å in TDO). A dative bond between the 2p orbital of the carbon atom (donor) and the sulfur atom (acceptor), as expected for a singlet carbene-like structure, can also be seen in these HOMOs.

2.4. *C−S bond cleavage in TDO*

C−S bond cleavage in TDO and FSA was examined in order to understand the mechanism of sulfoxylate generation: nominally, simple heterolytic cleavage of this bond would lead to an SO_2 moiety assignable as sulfoxylate. Figure 8 shows that when the C−S distance in TDO is

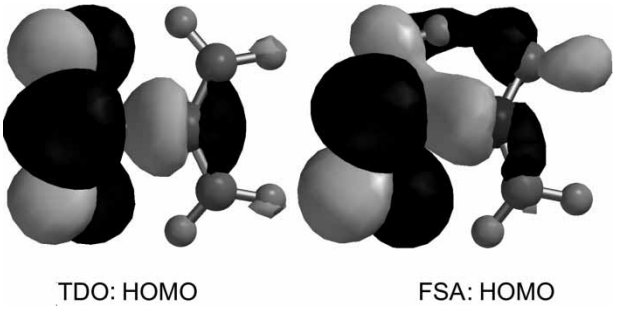

Figure 7. HOMO for TDO and FSA.

increased up to 4.3 Å (over 0.5 Å longer than the sum of sulfur + carbon van der Waals radii), a local minimum can be reached. However, the barrier for reverting this structure back to the starting TDO is negligible, which suggests that the C−S bond does not cleave by simply increasing the distance between these two atoms and that therefore this is not a viable mechanism for sulfoxylate formation.

Elongation of the C−S bond in FSA (Figure 9) yields similar results to the TDO C−S bond elongation discussed above. This is because at a C−S distance of approximately 2.4 Å, marked with a triangle in Figure 9, the oxygen-bound proton moves spontaneously to the nitrogen, so that FSA tautomerizes to TDO. From this point onwards, we enter the TDO potential energy surface covered by Figure 8, and again no feasible mechanism can be seen for sulfoxylate formation.

The effect of solvation on C−S bond cleavage in TDO was examined by placing 1 and then 10 molecules of water, without applying any constraints over them, in the vicinity of TDO (explicit solvation). No stabilization was observed at large C−S distances, corresponding to a state where the C−S bond is cleaved (data not shown).

The possibility of sulfoxylate formation as the result of a water molecule attacking the TDO carbon was also examined (*cf.* Figure 10); this reaction appears feasible energetically, even if the C−S bond does not break yet. However, to our knowledge, there is no experimental evidence for the Figure 10 reaction taking place, nor has the product been characterized. In fact, Figure 11 shows that this product would readily decompose to yield sulfoxylic acid. However, it is known experimentally that TDO is relatively stable in water and that its decomposition to sulfoxylate

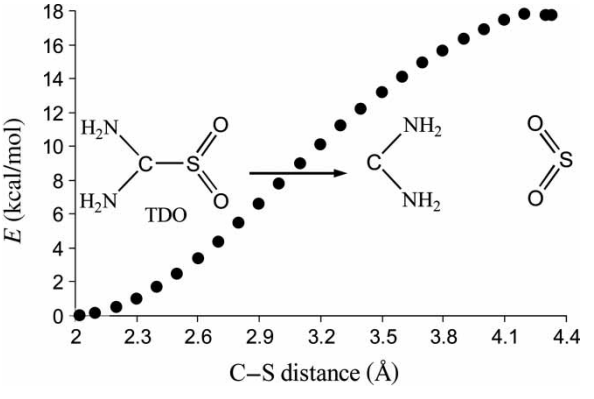

Figure 8. Evolution of the potential energy with the elongation of the C−S bond and rotation of the SO_2 moiety with O atoms toward the N-bound H atoms from TDO.

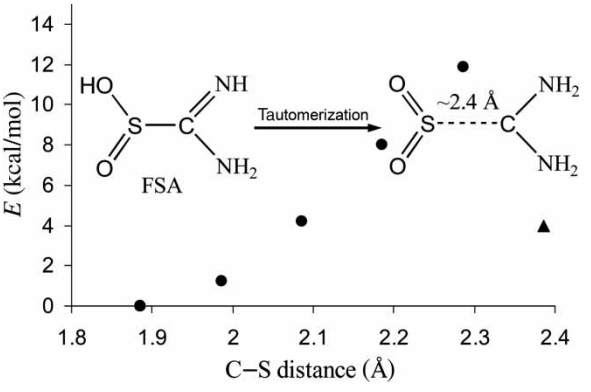

Figure 9. Evolution of the potential energy with the elongation of the C−S bond in FSA. At a C−S distance of 2.4 Å, FSA tautomerizes to TDO, represented by a triangle on the plot.

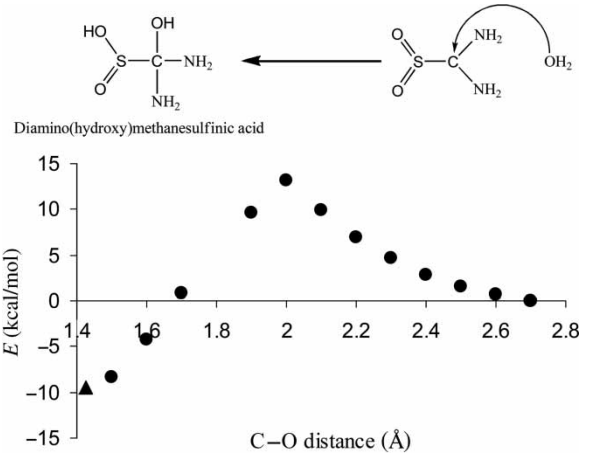

Figure 10. Potential curve for the attack of a water molecule over the carbon of TDO. The oxygen (water)−carbon (TDO) distance was varied as shown, while all other parameters were freely optimized.

proceeds only under basic medium with a pK_a of ~9; on the contrary, according to Figures 10 and 11, TDO decomposition to sulfoxylate should not have a significant pH dependence.

Figure 12 resolves the apparent conflict between the experimental and theoretical results of Figures 10 and 11: it is shown that the attack of a water molecule onto the carbon atom in the FSA tautomer of TDO is *not* energetically feasible: although a local minimum can be reached with a C (thiourea)−O (water) distance of ~1.6 Å, the barrier for returning to FSA and water is very small. Correlating with Figure 4 data, according to which FSA is more stable than TDO, these data led us to interpret that indeed the tautomer predominating in water at neutral and acidic medium is FSA rather than TDO. According to Figures 10–12, FSA should be water-stable but TDO less so.

As TDO generates sulfoxylate only in alkaline medium, cleavage of the C−S bond by elongating it in the presence of a hydroxide group was also examined (*cf.* Figure 13). The OH^- group was first placed at a distance of 3.5 Å from the carbon of TDO (further than the sum of van der Waals radii of oxygen and carbon). The OH group approaches spontaneously TDO in the initial point, before starting the elongation of the C−S bond, initial state in Figure 11. Elongating the C−S bond, with the $^-$OH bound to the carbon, the C−S bond cleaves; the potential curve is

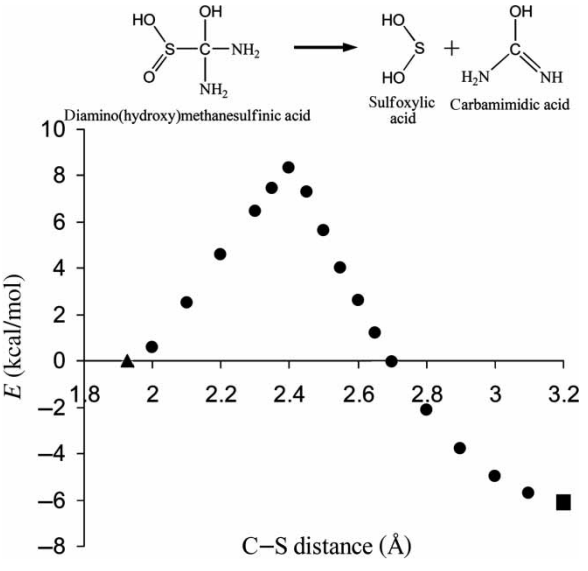

Figure 11. Decomposition of the putative TDO−water adduct produced in Figure 10, to yield sulfoxylic acid. The sulfur−carbon distance was varied as shown, while all other parameters were freely optimized.

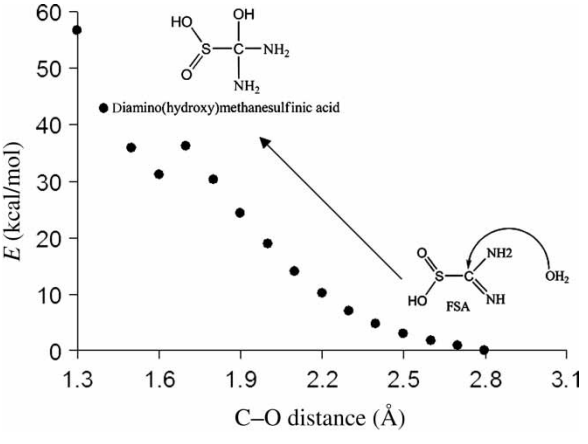

Figure 12. Potential energy surface for nucleophilic attack of a water molecule onto the carbon atom in FSA. The oxygen (water)−carbon (FSA) distance was varied as shown, while all other parameters were freely optimized.

represented by the black dots in Figure 11. This cleavage also occurs in the presence of a water molecule (gray squares) without any noticeable influence of the water molecule. However, this kind of C−S bond cleavage in TDO does not agree with experimental observations where a $pK_a \sim 9.5$ was determined. Moreover, the activation energy for the process (∼13 kcal/mol) is too low considering the experimentally observed TDO decomposition rate (*4, 5*). These results can again be interpreted, as was done above, to indicate that in water the TDO tautomer does not exist.

Elongation of C−S bond in nitrogen-deprotonated TDO (or oxygen-deprotonated FSA) was also considered, as it would fit with a scenario where the experimentally observed pK_a is assigned to TDO/FSA. As in the case of C−S bond elongation in neutral TDO and FSA, their deprotonated counterpart showed the energy increasing monotonously with the C−S distance and with no stable local minimum identifiable in the elongated structures (data not shown).

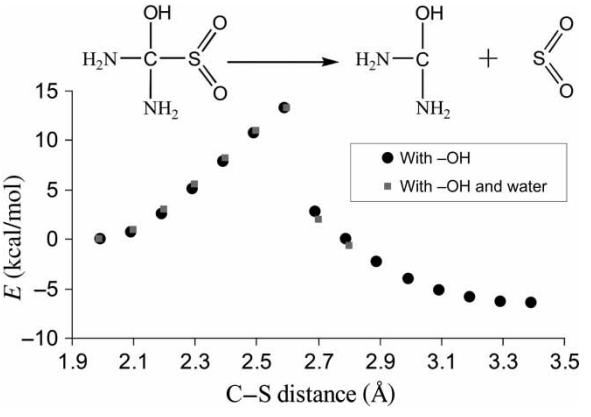

Figure 13. Variation of the energy with the elongation of the C−S bond in TDO after a $^{-}$OH group binds to the carbon in the presence and absence of a water molecule. The carbon−sulfur bond distance was varied as shown, while all other parameters were freely optimized.

Attack of the carbon atom in deprotonated TDO/FSA by water was also examined (*cf.* Figure 14). C−S bond cleavage occurs concerted with this attack, also concerted with transfer of a water proton to the sulfur-bound oxygen consistent with charge separation. Thus, the final product in this reaction scheme is indeed sulfoxylate, in good agreement with experiment.

The process shown in Figure 14 is not favorable thermodynamically. However, Figure 15 shows that subsequent isomerization of the nitrogen-containing moiety is in fact exothermic and can drive reaction in Figure 14 forward. The final point of the reaction path shown in Figure 4 shows a nitrogen−sulfur distance of 4.14 Å and a net charge on the SO_2H moiety, computed from NBO partial atomic charges, of −0.97, consistent with deprotonated sulfoxylate; the remaining organic part was urea, as indicated in Figure 15.

Based on these results, the following mechanism scheme is proposed for generation of sulfoxylate from TDO (*cf.* Figure 16). The first step includes deprotonation of TDO/FSA, followed

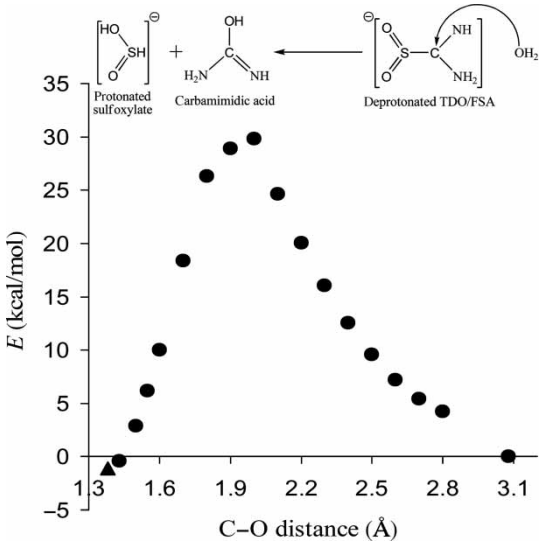

Figure 14. Potential curve for the attack of water to the carbon of deprotonated TDO/FSA. The oxygen (water)−carbon (FSA) distance was varied as shown, while all other parameters were freely optimized.

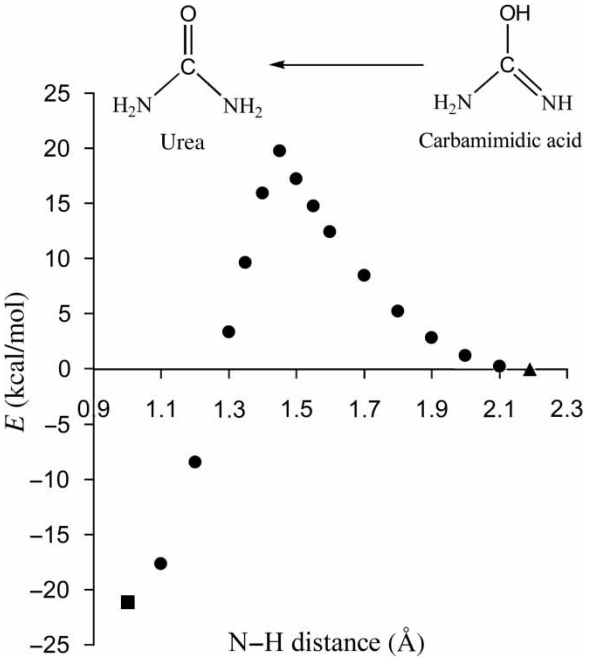

Figure 15. Potential curve for isomerization of carbamidic acid to urea. The distance between the oxygen-bound proton and the NH nitrogen was varied as shown, while all other parameters were maintained constant.

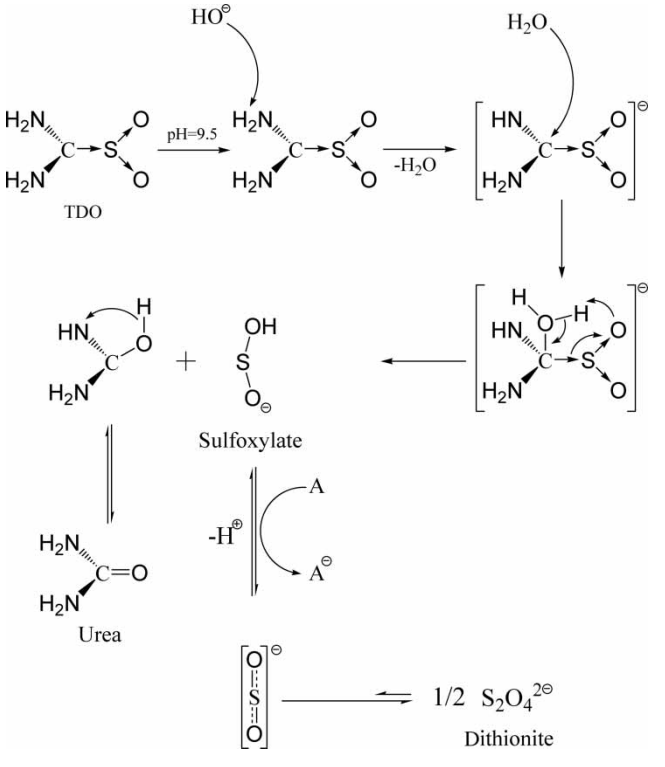

Figure 16. Proposed mechanism for sulfoxylate decomposition. 'A' is a generic electron acceptor.

by attack of water onto the carbon atom in a rate-limiting step during which carbon−sulfur bond cleavage also occurs, in concerted manner. Thus, two compounds are obtained from which one is the sulfoxylate, the other being readily isomerized to urea. Sulfoxylate will eventually be oxidized to dithionite.

Alternative mechanisms for sulfoxylate generation were also taken into consideration (not shown); among others, $^{-}$OH attack on the nitrogen or sulfur atoms in deprotonated TDO or water attack on the carbon of FSA deprotonated at the N was found to be unfeasible.

2.5. *Dioxygen liberation from TDO*

Paradoxically, besides liberating the extremely strong reducing agent sulfoxylate, TDO/FSA can, under certain conditions, also liberate dioxygen (*6*). Figure 17 shows that this process is indeed feasible. In line with the results shown in previous sections, this solution-phase property of TDO is easier explainable as due to the FSA tautomer, whose potential energy surface ion the critical regions (O−O distance between 1.3 and 1.7 Å) lies ∼100 kcal/mol below that of TDO. The significant difference in reactivity between the two tautomers is traceable to the oxygen-bound

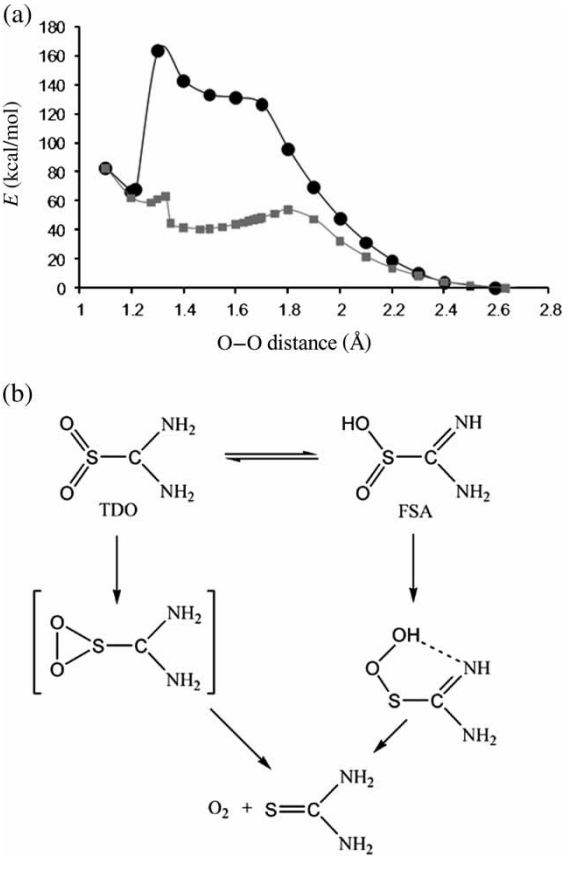

Figure 17. (a) Potential energy surface for dioxygen formation via O−O bond formation in TDO and its tautomer FSA (black and gray traces, respectively). The oxygen−oxygen distance was varied as shown, while all other parameters were freely optimized. (b) Reaction pathways for the two traces in (a): a local minimum featuring a hyproperoxide attached to the sulfur is identifiable as an intermediate on the FSA pathway, while no intermediate is identifiable on the TDO pathway.

proton in FSA, which allows partial stabilization of a peroxide S−O−O−H intermediate at an O−O distance of ∼1.5 Å in FSA.

In conclusion, the electronic structure of TDO and FSA was reconsidered in order to elucidate a TDO zwitterionic vs. carbenoid structure. Our data (molecular orbital analysis, charge distribution, C−S bond elongation) indicate that TDO has a carbenoid structure, in line with the interpretation proposed by Denk *et al.* (*14*). Intermolecular and intramolecular tautomerization mechanisms were both found feasible for interconversion of TDO to FSA. Mechanisms for TDO/FSA decomposition to yield sulfoxylate or dioxygen were also identified. All of the data points towards FSA being the dominant tautomer in aqueous solution, while TDO is stabilized by supramolecular interactions in solid state.

3. Experimental

Geometries were optimized using the B3LYP functional and the 6-31G** basis set as implemented in the Spartan software package (*15–17*). For the SCF calculations, a fine grid was used, and the convergence criteria were set to 10^{-6} (for the root-mean square of electron density) and 10^{-8} (energy), respectively. For geometry optimization, convergence criteria were set to 0.0005 a.u. (maximum gradient criterion) and 0.0003 (maximum displacement criterion). For selected models, similar results (not shown) were obtained within the Gaussian '98 package (*18*) at BP86/6-31G** and B3LYP/6-31G** levels. In cases where charge or spin separation was suspected, the unrestricted formalism was applied, but the results did not differ from those obtained with the restricted formalism. Frequencies were computed for stationary points to verify that they are true minima. NBO partial atomic charges are listed in tables.

The choice of the B3LYP functional is based on its widespread use, which would allow a more straightforward correlation of our results with those obtained by other groups on other systems. For the types of systems examined here, Siegbahn and co-workers and Noodleman and co-workers estimated errors as high as a few kcal/mol (*19–25*). One main alternative to the B3LYP employed here would be the non-hybrid BP86 functional; although the usefulness of BP86 in inorganic and bio-inorganic studies is documented (*25–31*), a hybrid functional was deemed to be a better choice since charge separation is sought in some of the reaction pathways examined here, and non-hybrid functionals do tend to underestimate such phenomena (*25, 30*). It may be argued that various newer functionals, which have not yet been applied extensively in bio-inorganic or bio-organic chemistry, may provide better results on structures or on energies (*32, 33*). However, as stated above, the use of such functionals would limit the possibilities of directly correlating our results with those obtained on other systems, by other groups. The possibility to establish trends, more than to compute single accurate values, is in our opinion the main strength of computational inorganic chemistry (*25*); such trends are difficult to establish unless any given computational approach gains widespread use. Nevertheless, as it is always important not to blindly trust 'mainstream' approaches, the performance of our model chemistry, B3LYP/6-31G**, was tested against a few other models, as shown in Table 3, looking at other functionals

Table 3. Performance of a few computational approaches on a test model (FSA–TDO tautomerization, as shown in Figure 4).

	From FSA	From TDO
G-B3lyp/6-31G**	2.8	1.8
G-B3LYP/6-31+G**	2.6	2.6
G-B1B95/6-31G**	3.1	2.1

as well as at a larger basis set. The results are in line with data already known: changing the functional can indeed alter the results by 1–2 kcal/mol, while changing the basis set has an even smaller effect.

Acknowledgements

Funding from a joint Russian Foundation for Basic Research/Romanian Academy (to S.V.M. and R.S.D.) as well as from the Romanian Government (Ideas project 565/2007 to R.S.D.) is gratefully acknowledged.

References

(1) Barnett, E.B. *J. Chem Soc.* **1910,** *97,* 63–65.
(2) Cegarra, J.; Gacen, J.; Caro, M.; Pepio, M. *J. Soc. Dyers Colour* **1988,** *104,* 273–279.
(3) Daneault, C.; Leduc, C. *Can. Cellul. Chem. Technol.* **1994,** *28,* 205–217.
(4) Makarov, S.V.; Kudrik, E.V.; van Eldik, R.; Naidenko, E.V. *J. Chem. Soc., Dalton Trans.* **2002,** 4074–4076.
(5) Makarov, S.V.; Salnikov, D.S.; Pogorelova, A.S.; Kis, Z. Silaghi-Dumitrescu, R. *J. Porph. Phthalocyan.* **2008,** *12,* 1096–1099.
(6) Burgess, E.M.; Zoller, U.; Burger, R.L. *J. Am. Chem. Soc.* **1984,** *106,* 1128–1130.
(7) Makarov, S.V. Unpublished observations.
(8) Kudrik, E.V.; Makarov, S.V.; Zahl, A.; van Eldik, R. *Inorg. Chem*. **2003,** *42,* 618–624.
(9) Kudrik, E.V.; Van Eldik, R.; Makarov, S.V. *J. Chem. Soc., Dalton Trans.* **2004,** 429–435.
(10) Kudrik, E.V.; Theodoridis, A.; van Eldik, R.; Makarov, S.V. *J. Chem. Soc., Dalton Trans*. **2005,** 1117–1122.
(11) Kudrik, E.; Makarov, S.V.; Zahl, A.; van Eldik, R. *Inorg. Chem.* **2005,** *44,* 6470–6475.
(12) Wang, Y.; Chang, N.-L.; Pai, C.-T. *Inorg. Chem.* **1990,** *29,* 3256–3259.
(13) Song, J.S.; Kim, E.H.; Kang, S.K.; Yun, S.S.; Suh, I.-H.; Choi, S.-S.; Lee, S.; Jensen, W.P. *Bull. Korean Chem. Soc.* **1996,** *17,* 201–205.
(14) Denk, M.K.; Hatano, K.; Lough, A.J. *Eur. J. Inorg. Chem.* **2003,** 224–231.
(15) Becke, A.D. *Phys. Rev.* **1988,** 3098–3100.
(16) Perdew, J.P. *Phys. Rev.* **1986,** *B33,* 8822–8824.
(17) Wavefunction, Inc. *Spartan 5.0*, Wavefunction, Inc., USA.
(18) Frisch, M.J.; Trucks, G.W.; Schlegel, H.B.; Scuseria, G.E.; Robb, M.A.; Cheeseman, J.R.; Zakrzewski, V.G.; Montgomery, J.A.; Stratmann, R.E.; Burant, J.C.; Dapprich, S.; Millam, J.M.; Daniels, A.D.; Kudin, K.N.; Strain, M.C.; Farkas, O.; Tomasi, J.; Barone, V.; Cossi, M.; Cammi, R.; Mennucci, B.; Pomelli, C.; Adamo, C.; Clifford, S.; Ochterski, J.; Petersson, G.A.; Ayala, P.Y.; Cui, Q.; Morokuma, K.; Malick, D.K.; Rabuck, A.D.; Raghavachari, K.; Foresman, J.B.; Cioslowski, J.; Ortiz, J.V.; Stefanov, B.B.; Liu, G.; Liashenko, A.; Piskorz, P.; Komaromi, I.; Gomperts, R.; Martin, R.L.; Fox, D.J.; Keith, T.; Al-Laham, M.A.; Peng, C.Y.; Nanayakkara, A.; Gonzalez, C.; Challacombe, M.; Gill, P.M.W.; Johnson, B.G.; Chen, W.; Wong, M.W.; Andres, J.L.; Head-Gordon, M.; Replogle, E. S.; Pople, J.A. *Gaussian '98 (Revision A.1)*, Gaussian, Inc., Pittsburgh, PA, 1998.
(19) Siegbahn, P.E.M.; Blomberg, M.R.A. *Chem. Rev.* **2000,** *100,* 421–437.
(20) Siegbahn, P.E.M.,Blomberg, M.R.A. *Annu. Rev. Phys. Chem.* **1999,** *50,* 221–249.
(21) Himo, F.; Siegbahn, P.E. *Chem. Rev*. **2003,** *103,* 2421–2456.
(22) Blomberg, L.M.; Blomberg, M.R.A.; Siegbahn, P.E.M. *J. Biol. Inorg. Chem.* **2004,** *9,* 923–935.
(23) Bassan, A.; Borowski, T.; Siegbahn, P.E. *J. Chem. Soc., Dalton Trans*. **2004,** 3153–3162.
(24) Noodleman, L.; Lovell, T.; Han, W.G.; Li, J.; Himo, F. *Chem. Rev*. **2004,** *104,* 459–508.
(25) Silaghi-Dumitrescu, R.; Silaghi-Dumitrescu, I. *Chemtracts Inorg. Chem.* **2005,** *18,* 595–619.
(26) Silaghi-Dumitrescu, R. *Inorg. Chem.* **2004,** *43,* 3715–3718.
(27) Silaghi-Dumitrescu, R. *Eur. J. Inorg. Chem.* **2003,** 1048–1052.
(28) Silaghi-Dumitrescu, R.; Cooper, C.E. *J. Chem. Soc., Dalton Trans.* **2005,** 3477–3482.
(29) Silaghi-Dumitrescu, R. *J. Biol. Inorg. Chem.* **2004,** *9,* 471–476.
(30) Silaghi-Dumitrescu, R.; Silaghi-Dumitrescu, I. *J. Inorg. Biochem.* **2006,** *100,* 161–166.
(31) Silaghi-Dumitrescu, R. *Eur. J. Inorg. Chem.* **2008,** 5404–5407.
(32) Leverentz, H.R.; Truhlar, D.G. *J. Phys. Chem. A* **2008,** *112,* 6009–6016.
(33) Zhao, Y.; Truhlar, D.G. *J. Phys. Chem. A* **2005,** *109,* 5656–5667.